NASA Technical Paper 2920

1989

Kaon-Nucleus Scattering

Byungsik Hong and
Khin Maung Maung
Hampton University
Hampton, Virginia

John W. Wilson
Langley Research Center
Hampton, Virginia

Warren W. Buck
Hampton University
Hampton, Virginia

National Aeronautics and
Space Administration
Office of Management
Scientific and Technical
Information Division

Contents

Abstract

The derivations of the Lippmann-Schwinger equation and the Watson multiple-scattering series are given. A simple optical potential is found to be the first term of that series. The number density distribution models of the nucleus, harmonic well and Woods-Saxon, are used with our t-matrix taken from the scattering experiments. The parameterized two-body inputs, which are kaon-nucleon total cross sections, elastic slope parameters, and the ratio of the real to the imaginary part of the forward elastic scattering amplitude, are presented. The eikonal approximation was chosen as our solution method to estimate the total and absorptive cross sections for the kaon-nucleus scattering.

1. Introduction

The scattering of a high energy incoming particle, particularly a meson, by the nucleus can be considered in terms of its scattering by the constituent nucleons of the nucleus individually. This means that the many-body interaction may be reduced to a combination of two-body interactions. Thus, naturally, the mathematical form for these two-body amplitudes as well as the detailed knowledge of the basic two-body input is necessary. Even though a number of models have been used to treat these kinds of problems, it is still one of the essential tasks of medium energy physics to understand how the basic meson-nucleon amplitudes can be extended to the many-body problem.

One of the successful scattering frameworks is the multiple-scattering theory. A simple picture of the scattering of elementary particles by a nucleus is to view the scattering in terms of the projectile interactions with each single constituent of the nucleus (single scattering). There may be other terms contributing to the scattering such as the projectile interacting consecutively with two different constituents (double scattering). Similarly there are contributions from three, four, and more successive scatterings. The formalisms using this picture are called *multiple-scattering theories* (refs. 1, 2, and 3). From this description, the scattering from a nucleus is determined from the amplitude for the scattering of the projectile from a single target constituent, that is, a two-body scattering amplitude (ref. 4).

On the other hand, a useful device for the analysis of particle scattering experiments is the optical model. Historically, Fernbach, Serber, and Taylor (ref. 5) have considered the nucleus to be a continuous optical medium characterized by the index of refraction and an absorption coefficient in their study of the scattering of high energy neutrons by nuclei. The phase shift of the incident wave was calculated as if it had followed a well-defined geometric path through the nucleus, and the total wave was the algebraic sum of the wavelets resulting from all paths. The fact that the optical potentials are complex is worth noticing. The name *optical potential* was chosen because of its analogy with the propagation of light through a semitransparent medium which has a complex index of refraction. The imaginary part of the optical potential corresponds to absorption of the incident beam by the medium (ref. 4), and the real part of the optical potential corresponds to the refraction of the beam without any disturbance of the medium. The multiple-scattering theory is useful in defining an optical model. This allows the optical potential for elementary particle scattering from a nucleus to be determined from more fundamental quantities as the two-body scattering amplitude and the target number density function.

A general multiple-scattering theory for scattering of two composite nuclei (neglecting three-body interactions) has previously been developed by Wilson (refs. 4 and 6). The reaction for the heavy ion projectile, which is the previous application of Wilson's theory, was well developed by Wilson and Townsend (ref. 7). The applications to the antiproton, antideuteron, and antinuclei were done by Buck, Norbury, Townsend, and Wilson (refs. 8 and 9) giving good agreement with the experimental data.

The purpose of this work is to estimate the total and absorptive (absorption) cross sections for the kaon-nucleus systems from the kaon-nucleon information. The starting point is the

Schrödinger equation, which is time independent with a many-body potential. The Lippmann-Schwinger equation, which is an integral form of the Schrödinger equation with the scattering boundary condition in terms of the optical potential operator, is derived, and the optical potential operator is given by the Watson multiple-scattering series. The relations at high energies are simpler than the low energy scattering in many respects. This is why we may adopt the impulse approximation which considers only the free t-matrix and ignores effects arising from other components. When only two-body interactions are considered and the impulse approximation at high energies is assumed, we get the simplified optical potential.

Owing to the paucity of the experimental data for kaon-nucleus scattering, we cannot calculate how much our results deviate from experiment. There are insufficient kaon data because of the difficulty in producing a kaon projectile beam. However, comparing the differential cross sections for the kaon-proton system at several energies and for the kaon-carbon system at a kaon laboratory momentum of 800 MeV/c (where c is the velocity of light) confirms that our results are reasonable.

2. Theoretical Formulation

The total Hamiltonian H satisfies the time-independent Schrödinger equation

$$H|\Psi\rangle = E|\Psi\rangle \tag{2.1}$$

where E is the eigenvalue of operator H and $|\Psi\rangle$ is the state vector. In the case of projectile-nucleus scattering, the total Hamiltonian is given by

$$H = H_0 + V \tag{2.2}$$

where

$$H_0 = h_0 + H_A \tag{2.3}$$

is the unperturbed or free Hamiltonian of the scattering system, and the residual interaction is given by

$$V = \sum_{i=1}^{A} v_{0i} \tag{2.4}$$

The operator v_{0i} is the potential energy operator between the projectile and ith target constituent. Here h_0 is the kinetic energy operator of the projectile, and

$$H_A = \sum_{i=1}^{A} h_i + \sum_{i<j} v_{ij} \tag{2.5}$$

is the target Hamiltonian. The kinetic energy operator h_i is the projectile kinetic energy for the ith target component, and the potential energy operator v_{ij} is for the potential between ith and jth target components.

Equation (2.1) is now

$$(H_0 + V)|\Psi\rangle = E|\Psi\rangle \tag{2.6}$$

The eigen equation for the target is

$$H_A|\phi_A^n\rangle = E_A^n|\phi_A^n\rangle \tag{2.7}$$

and the target ground state is given by $|\phi_A^0\rangle$. The unperturbed Hamiltonian H_0 satisfies

$$H_0|\phi\rangle = E|\phi\rangle \tag{2.8}$$

where $|\phi\rangle$ is the product state of the projectile plane wave state $|k\rangle$ and the target ground state $|\phi_A^0\rangle$; that is, $|\phi\rangle \equiv |\phi_A^0\rangle|k\rangle$.

The two differential equations (eqs. (2.6) and (2.8)) can be combined with the scattering boundary condition and can be written as an integral equation; that is,

$$|\Psi^{\pm}\rangle = |\phi\rangle + G_0^{\pm} V |\Psi^{\pm}\rangle \tag{2.9}$$

In this equation, the Green's function $G_0^{\pm}$ is given by

$$G_0^{\pm}(E \pm i\eta) = (E - H_0 \pm i\eta)^{-1} \tag{2.10}$$

where the superscript + represents the outgoing state and the superscript − denotes the incoming state, but these superscripts are omitted hereafter. Equation (2.9) is the Lippmann-Schwinger equation for $|\Psi\rangle$ (refs. 10 and 11).

We define a transition operator T such that

$$T|\phi\rangle = V|\Psi\rangle \tag{2.11}$$

Operating with V from the left on equation (2.9), we get

$$T|\phi\rangle = V|\phi\rangle + VG_0T|\phi\rangle \tag{2.12}$$

Therefore we get the operator form of the Lippmann-Schwinger equation for T,

$$T = V + VG_0T \tag{2.13}$$

It is not economical to solve directly the Lippmann-Schwinger equation in the form given by equation (2.13) because it is a many-body equation and its matrix element can be infinite in the case of hard core potential. We must therefore reduce it to an effective one-body equation to solve the Lippmann-Schwinger equation.

The first step in defining an effective one-body equation is to define the target ground state projectile operator as

$$P = |\phi_A^0\rangle\langle\phi_A^0| \tag{2.14}$$

and the closure relation as

$$Q = 1 - P \tag{2.15}$$

Using equation (2.15), the Lippmann-Schwinger equation (2.13) can be written as two coupled equations:

$$T = W + WPG_0PT \tag{2.16}$$

and

$$W = V + VQG_0QW \tag{2.17}$$

where W is the optical potential operator. Note that equations (2.16) and (2.17) together represent exactly the same physics as equation (2.13). Equation (2.16) is an effective one-body equation after taking the target matrix elements. Actually we do not get much by rewriting equation (2.13) as coupled equations (2.16) and (2.17), since the many-body nature of the problem still persists in equation (2.17), and the matrix element of equation (2.17) may still diverge for singular interactions. At this stage we employ the multiple-scattering formalism first introduced by Watson (ref. 1). We write W as

$$W = \sum_{i=1}^{A} w_{0i} \tag{2.18}$$

Equation (2.17) can be resummed as

$$W = \sum_{i=1}^{A} \tau_{0i} + \sum_{i=1}^{A} \tau_{0i} QG_0Q \sum_{j \neq i} \tau_{0j} + \ldots \tag{2.19}$$

where

$$\tau_{0i} = v_{0i} + v_{0i} Q G_0 Q \tau_{0i}$$
$$= v_{0i} + \tau_{0i} Q G_0 Q v_{0i} \tag{2.20}$$

Equation (2.19) is the Watson multiple-scattering series for the optical potential operator. And by keeping the first term only, we obtain the first-order optical potential. The τ operator in equations (2.19) and (2.20) is not a free two-body t-matrix because of the presence of QG_0Q in equation (2.20). The operator τ is related to the free two-body t-matrix by

$$\tau_{0i} = t_{0i} + t_{0i}(QG_0Q - g)\tau_{0i} \tag{2.21}$$

where the free t-matrix is given by

$$t_{0i} = v_{0i} + v_{0i} g t_{0i} \tag{2.22}$$

and

$$g = (E - h_o + i\eta)^{-1} \tag{2.23}$$

Moreover, if we impose the impulse approximation, which means that we consider the interaction only between projectile and each constituent of the target nucleus and neglect the effects from other target components at high energies, we will obtain a very simple expression for the optical potential operator

$$W = \sum_{i=1}^{A} t_{0i} \tag{2.24}$$

If we want to put in corrections to this impulse-approximated optical potential, we must consider two terms. The first one is due to the differences between QG_0Q and g in equation (2.21), known as the propagator correction. The second one is the double scattering term in equation (2.19). Since both of them are quadratic in the scattering operator, we should consider both corrections at the same time. The study of these corrections is being undertaken by Khin Maung Maung, Lawrence W. Townsend, and Philip A. Deutchman at the Langley Research Center.

To solve equation (2.16), we need the matrix element of W; that is,

$$W = \langle k' | \langle \phi_A^0 | W | \phi_A^0 \rangle | k \rangle \tag{2.25}$$

or

$$A \langle k' | \langle \phi_A^0 | t_{0i} | \phi_A^0 \rangle | k \rangle \tag{2.26}$$

where A is the atomic number of the target nucleus. By considering that the range of t is small compared with the size of the nucleus and using the factorization approximation, we obtain the $t\rho$ approximation for the optical potential as

$$W(q) = A\ t(q)\ \rho_A(q) \tag{2.27}$$

where

$$q = |k' - k| \tag{2.28}$$

is the momentum transfer and ρ_A is defined as

$$\rho_A(q) = \int \phi^*(p,q)\ \phi(p,q)\ dp \tag{2.29}$$

Now writing the expression for W as in equation (2.27), we can solve equation (2.16) by the method of partial waves. But we are mainly interested in the total and absorptive cross

sections in kaon-nucleus scattering for a large number of energies with a variety of targets. Computationally, the use of an appropriate approximation method is more economical. For this work, we chose the eikonal approximation as our solution method (ref. 11). In the eikonal context, the scattering amplitude for the kaon-nucleus scattering is given by

$$f(k,\theta) = \frac{k}{2\pi i}\int d^2b\ \exp(i\mathbf{q}\cdot\mathbf{b})\left\{\exp[i\chi(\mathbf{b},k)] - 1\right\} \tag{2.30}$$

where

$$\chi(\mathbf{b},k) = -\frac{1}{2k}\frac{2\mu}{\hbar^2}\int_{-\infty}^{\infty} W(\mathbf{b},z)\,dz \tag{2.31}$$

is the eikonal scattering phase shift function, $\mathbf{b}$ is the impact parameter, $\hbar$ is the Planck's constant divided by 2π, and μ is the reduced mass of the kaon-nucleus system. Using this scattering amplitude (eq. (2.30)) and the optical theorem, we can obtain the total and absorption cross sections expressed as follows:

$$\sigma_{\text{total}} = 2\int d^2b\,\left(1 - \exp\{-\text{Im}[\chi(\mathbf{b},k)]\}\cos\text{Re}[\chi(\mathbf{b},k)]\right) \tag{2.32}$$

and

$$\sigma_{\text{absorption}} = \int d^2b\,\left(1 - \exp\{-2\text{Im}[\chi(\mathbf{b},k)]\}\right) \tag{2.33}$$

3. Optical Potential

The number density ρ_A of nuclear matter can be extracted from the corresponding charge density ρ_C by assuming (ref. 7)

$$\rho_C(r) = \int \rho_N(r')\,\rho_A(r+r')\,d^3r' \tag{3.1}$$

where ρ_C is the nuclear charge distribution, ρ_N is the nucleon charge distribution, and ρ_A is the nuclear single-particle density. In equation (3.1), it was assumed that

$$\rho_N(r) = \rho_p(r) \tag{3.2}$$

where ρ_p is the proton charge distribution. The distribution ρ_N was taken to be the usual Gaussian function

$$\rho_N(r) = \left(\frac{3}{2\pi r_N^2}\right)^{3/2}\exp\left(-\frac{3r^2}{2r_N^2}\right) \tag{3.3}$$

with a nucleon root-mean-square charge radius r_N set equal to the proton value of 0.87 fm (ref. 8).

For nuclei with $A < 20$, we used a harmonic well form of ρ_C as

$$\rho_C(r) = \rho_0\left[1 + \gamma\left(\frac{r}{a}\right)^2\right]\exp\left(-\frac{r^2}{a^2}\right) \tag{3.4}$$

where the charge distribution parameters γ and a are given in table 3.1. Substituting equations (3.3) and (3.4) into equation (3.1), we get

$$\rho_A(r) = \frac{\rho_0 a^3}{8s^3}\left[1 + \frac{3\gamma}{2} - \frac{3\gamma a^2}{8s^2} + \frac{\gamma a^2 r^2}{16s^4}\right]\exp\left(-\frac{r^2}{4s^2}\right) \tag{3.5}$$

where

$$s^2 = \frac{a^2}{4} - \frac{r_N^2}{6} \tag{3.6}$$

The normalization coefficient ρ_0 can be calculated directly by

$$\rho_0 = \frac{1}{\pi^{3/2}a^3}\left(1 + \frac{3\gamma}{2} - \frac{3\gamma a^2}{8s^2} + \frac{3\gamma a^2}{8s^2}\right)^{-1} \tag{3.7}$$

For target nucleus with $A \geq 20$, we chose a Woods-Saxon form of charge distribution as follows:

$$\rho_C(r) = \rho_0\left[1 + \exp\left(\frac{r-R}{c}\right)\right]^{-1} \tag{3.8}$$

where the parameters R and c are given by

$$R = r_{0.5} \tag{3.9}$$

and

$$c = \frac{t_c}{4.4} \tag{3.10}$$

and $r_{0.5}$ is the radius at half-density with t_c representing the skin thickness. Values for R and t_c are taken from reference 8 and also shown in table 3.1. If we substitute equations (3.3) and (3.8) into equation (3.1), we see the nuclear single-particle density that is also of Woods-Saxon form with the same R, but a different normalization coefficient ρ_0 and surface thickness; that is (ref. 8),

$$\rho_A(r) = \rho_{A0}\left[1 + \exp\left(\frac{r-R}{c_A}\right)\right]^{-1} \tag{3.11}$$

where

$$c_A = \frac{t_A}{4.4} = 1.16 r_N\left[\ln\left(\frac{3\beta - 1}{3 - \beta}\right)\right]^{-1} \tag{3.12}$$

and

$$\beta = \exp\left(2.54\frac{r_N}{t_c}\right) \tag{3.13}$$

The overall normalization factor ρ_{A0} is given by

$$\rho_{A0} = \frac{3}{4\pi(R^3 + \pi^2 c_A^2 R)} \tag{3.14}$$

We chose the kaon-nucleon scattering amplitude to be the function of momentum transfer q as

$$f(q) = \frac{k}{4\pi}\sigma_T(i + \alpha)\exp\left(-\frac{Bq^2}{2}\right) \tag{3.15}$$

where k is the wavenumber of the kaon-nucleon system, σ_T is the kaon-nucleon total cross section, α is the ratio of the real part to the imaginary part of the forward elastic scattering, and B is the slope parameter. It should be noticed that the form of $f(q)$ was chosen to satisfy the optical theorem. Then the t-matrix in the coordinate space is

$$t(r) = -\sqrt{\frac{e\hbar^2}{2\mu'}}\sigma_T(i + \alpha)\frac{1}{(2\pi B)^{3/2}}\exp\left(-\frac{r^2}{2B}\right) \tag{3.16}$$

where e is the total kinetic energy in the center-of-mass frame, μ' is the reduced mass of the colliding particles, and $\hbar$ is the Planck's constant divided by 2π. The parameters σ_T, α, and B

used in equation (3.16) are parameterized as a function of kaon incident energy. The details of the fitting procedure of those quantities are given in section 4.

We compared our scattering amplitude (eq. (3.15)) with the experimental data of the K^+-p differential cross section taken from reference 12 and show the results in figures 3.1 through 3.7. We followed the plotted parameters of reference 12. The relation between the scattering amplitude and the differential cross section is

$$\frac{d\sigma}{d\Omega} = |f(k,\theta)|^2 \tag{3.17}$$

In the case of the kaon-nucleus scattering, the present calculation utilizing eikonal scattering amplitude (eq. (2.30)) and the experimental data (ref. 13) for C^{12} are displayed in figures 3.8 and 3.9.

From these results, we might conclude that the parameterization of the t-matrix is quite reasonable. The optical potentials based on the above information for K^+ and K^- projectiles and C^{12} target are shown in figures 3.10 and 3.11.

Table 3.1. Nuclear Charge Distribution Parameters From Electron Scattering
Data From Reference 8

Nucleus	Distribution (a)	γ or t_c, fm	a or R, fm
H^2	HW	0.000	1.710
He^4	HW	0.000	1.330
Li^7	HW	0.327	1.770
Be^9	HW	0.611	1.791
B^{11}	HW	0.811	1.690
C^{12}	HW	1.247	1.649
N^{14}	HW	1.291	1.729
O^{16}	HW	1.544	1.833
Ne^{20}	WS	2.517	2.740
Al^{27}	WS	2.504	3.050
Ar^{40}	WS	2.693	3.470
Fe^{56}	WS	2.611	3.971
Cu^{64}	WS	2.504	3.050
Br^{80}	WS	2.306	4.604
Ag^{108}	WS	2.354	5.139
Ba^{138}	WS	2.621	5.618
Pb^{208}	WS	2.416	6.624

[a]HW denotes harmonic well distributions; WS denotes Woods-Saxon distributions.

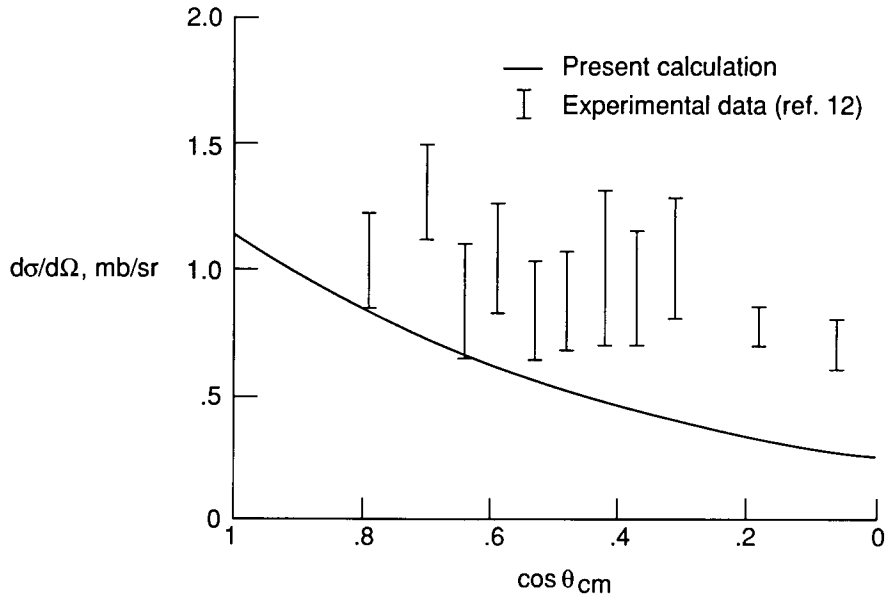

Figure 3.1. Differential cross section of K^+-p scattering at 503 MeV as function of center-of-mass scattering angle.

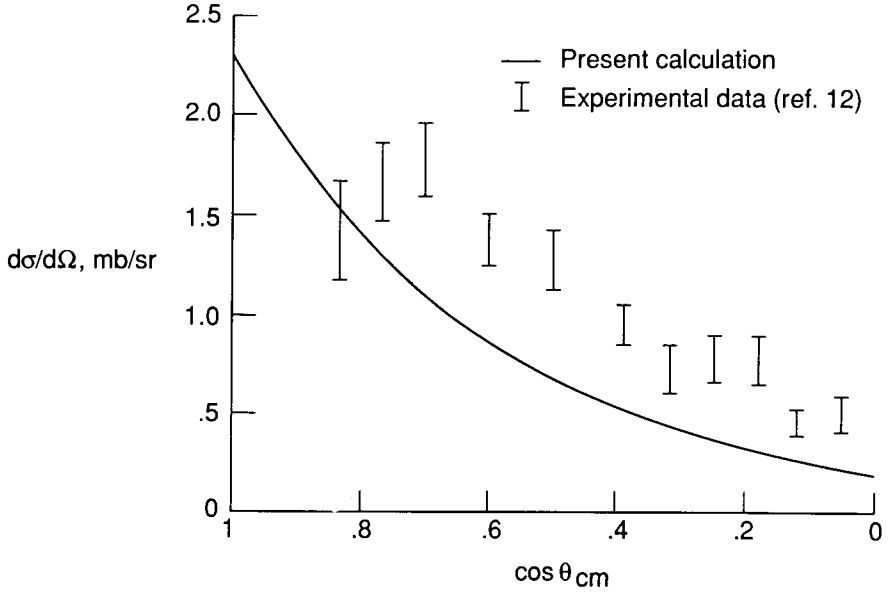

Figure 3.2. Differential cross section of K^+-p scattering at 820 MeV as function of center-of-mass scattering angle.

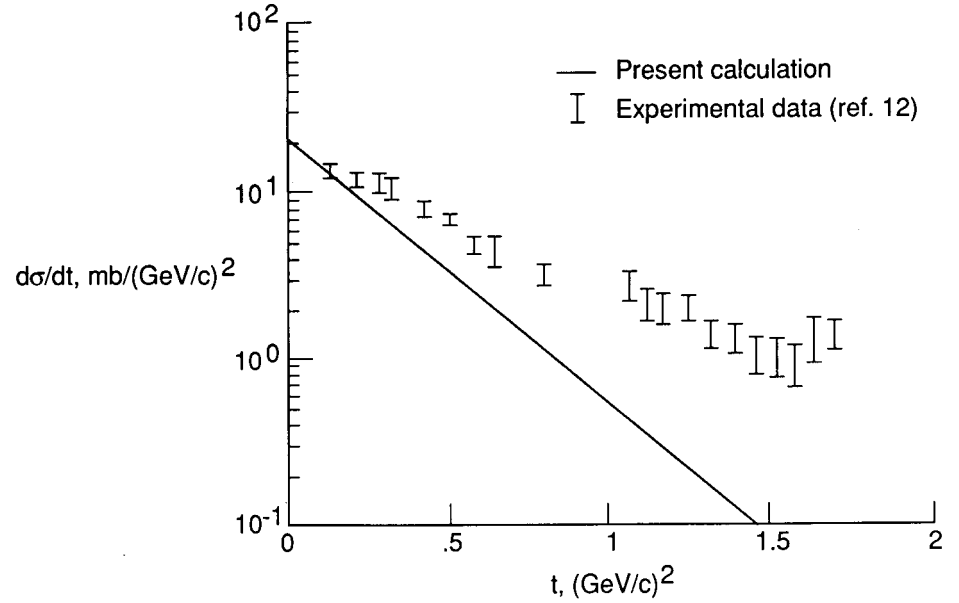

Figure 3.3. Differential cross section of K^+-p scattering at 1041.4 MeV as function of momentum transform squared.

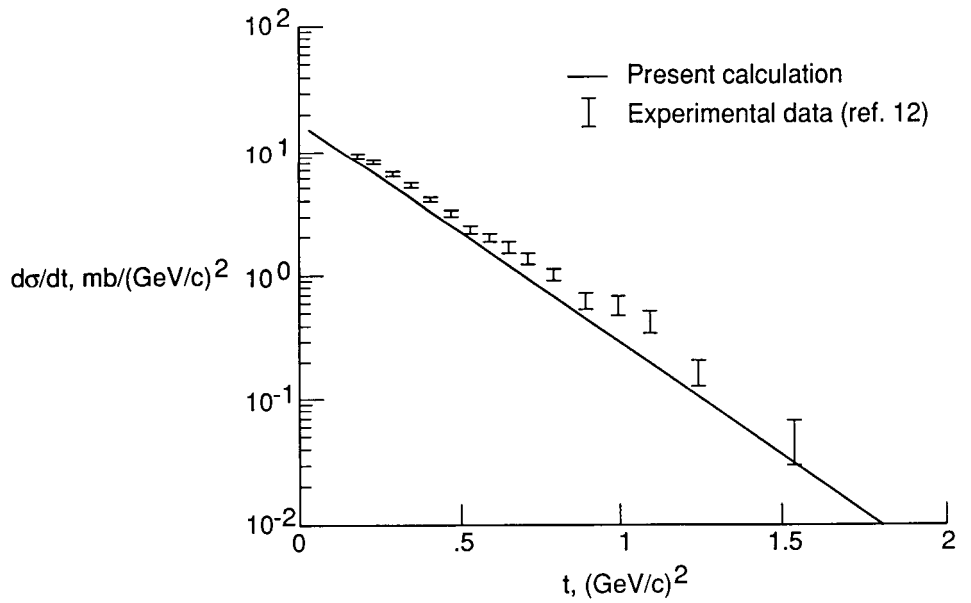

Figure 3.4. Differential cross section of K^+-p scattering at 3091 MeV as function of momentum transform squared.

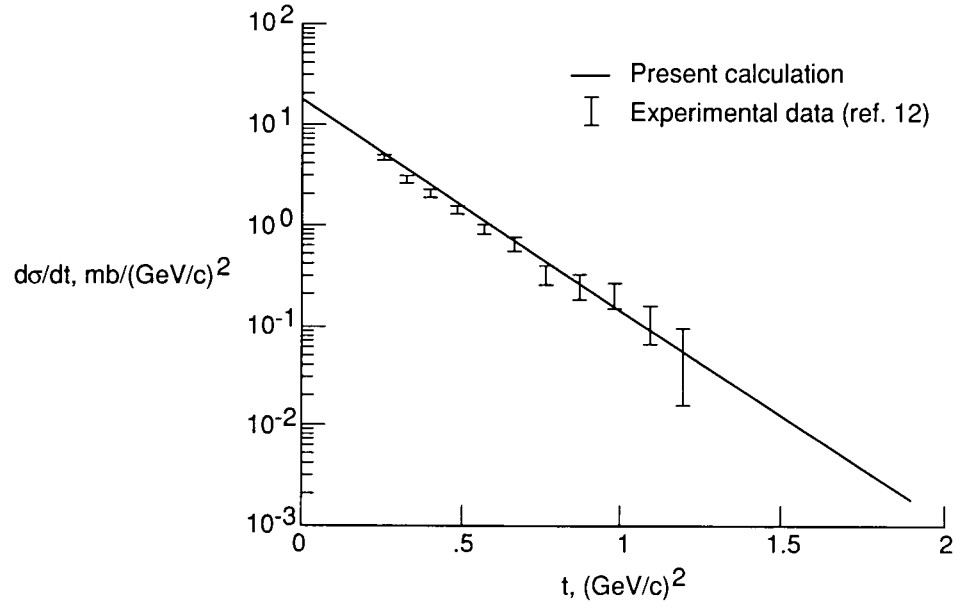

Figure 3.5. Differential cross section of K^+-p scattering at 6324.9 MeV as function of momentum transform squared.

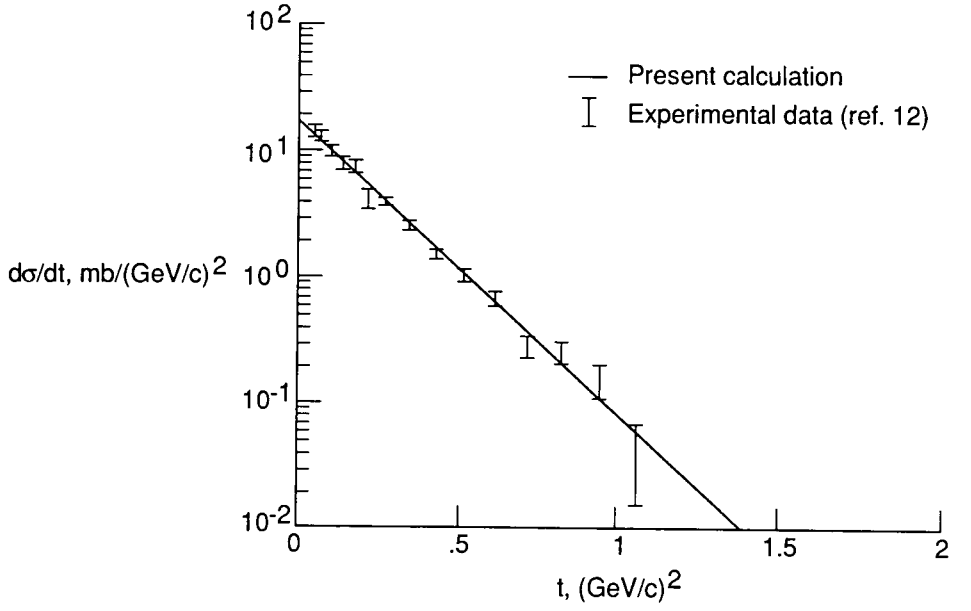

Figure 3.6. Differential cross section of K^+-p scattering at 9319.4 MeV as function of momentum transform squared.

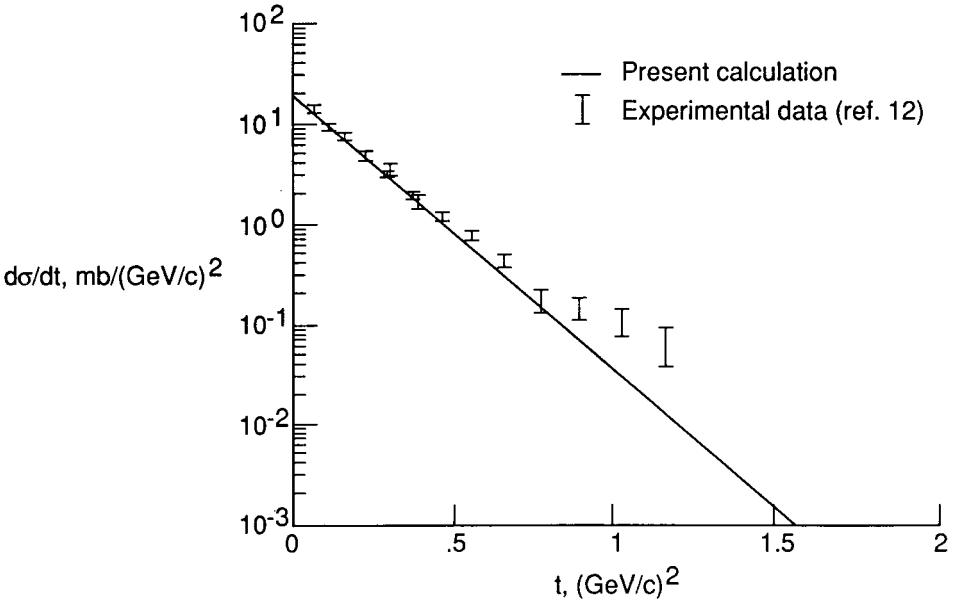

Figure 3.7. Differential cross section of K^+-p scattering at 14.3 GeV as function of momentum transform squared.

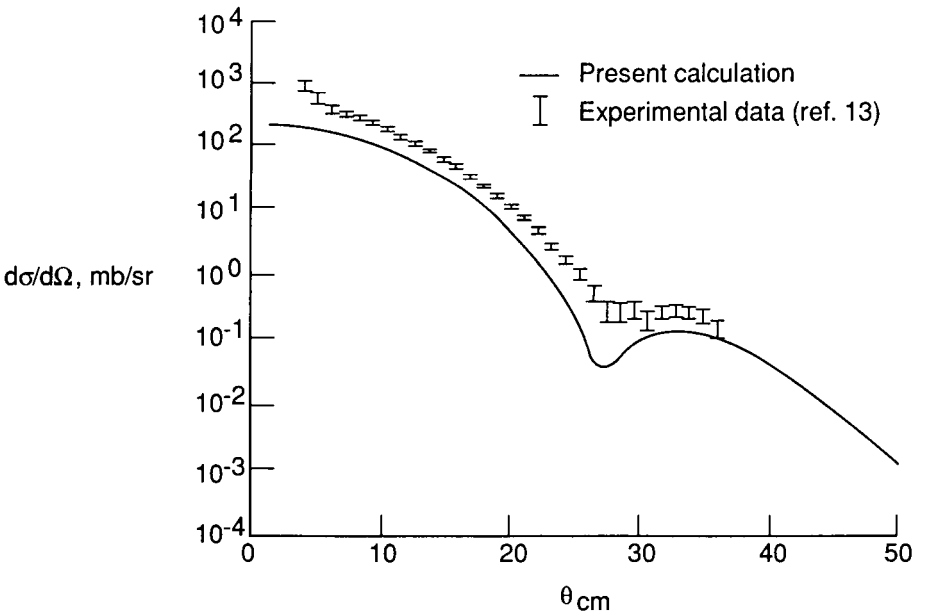

Figure 3.8. Differential cross section of K^+-C^{12} scattering at 800 MeV as function of center-of-mass scattering angle.

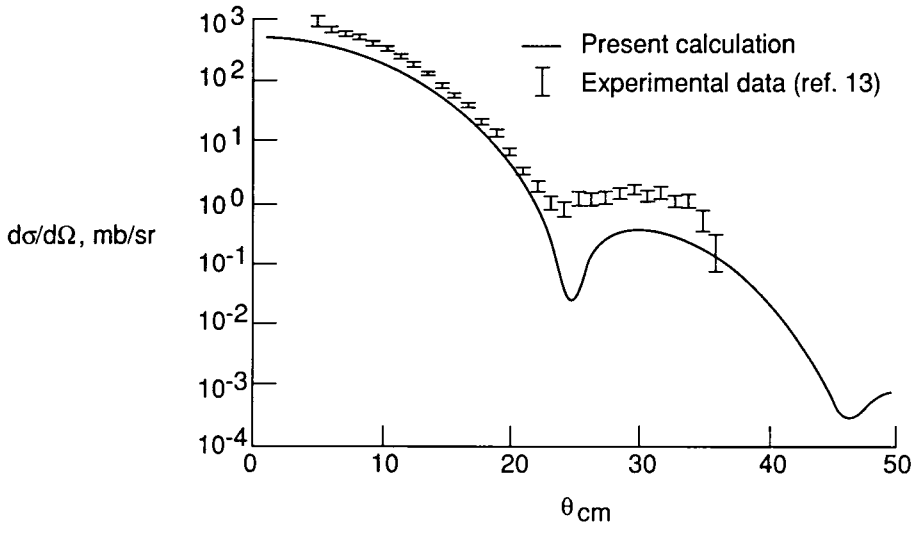

Figure 3.9. Differential cross section of K^--C^{12} scattering at 800 MeV as function of center-of-mass scattering angle.

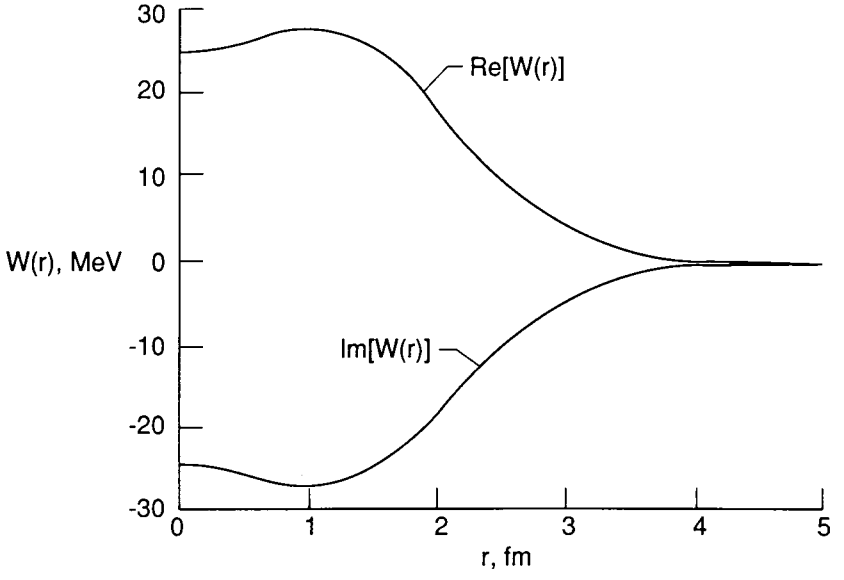

Figure 3.10. K^+-C^{12} optical potential at 800 MeV/c.

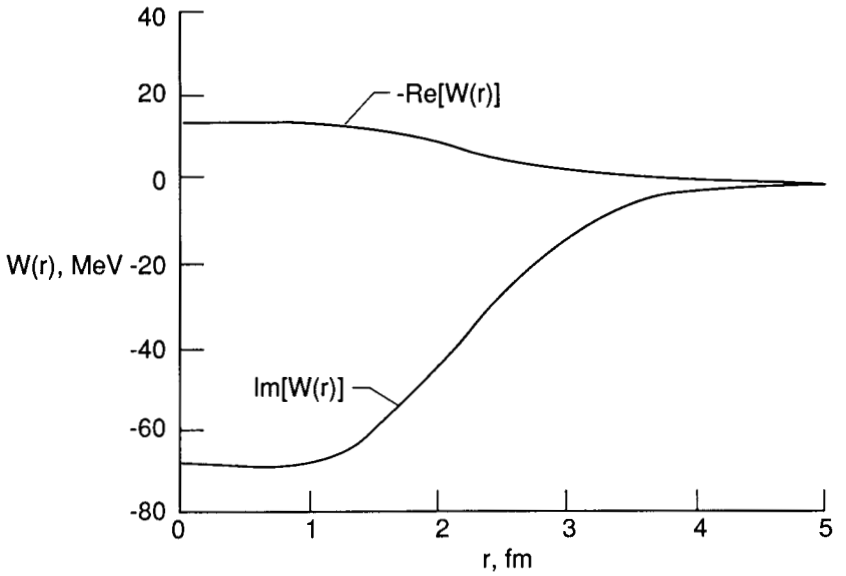

Figure 3.11. K^--C^{12} optical potential at 800 MeV/c.

4. Two-Body Input Parameters

4.1. Total Cross Section of Kaon-Nucleon System

The total cross sections of the K^+-p and K^--p scattering are approximated over two energy regions like most other elementary particle scattering amplitudes. The total cross sections are characterized by several peaks in the relatively low energy resonance region. However, the heights of the peaks decrease with increasing energy, and these peaks, eventually, show smooth behavior in the high energy region for the larger momenta. In the former region, the cross sections are determined according to the type of colliding particles. In the latter region, these dependencies disappear gradually. The K^--p total cross section presents a number of resonance peaks, but the K^+-p total cross section displays only a few structures. The interpretation of these resonances is unsettled at present (ref. 14).

Both these total cross sections may be fitted by the following form:

$$\sigma_T = \sigma_b(P_{K,\text{lab}}) + \sum_i g_i(P_{K,\text{lab}}) \tag{4.1}$$

where $P_{K,\text{lab}}$ is the corresponding kaon laboratory momentum in GeV/c and the unit of σ is mb. The typical form of $g_i(P_{K,\text{lab}})$ is that

$$g_i(P_{K,\text{lab}}) = \frac{m_i}{\left[(P_{R,i} - P_{K,\text{lab}})\,\frac{2}{n_i}\right]^2 + 1} \tag{4.2}$$

where $P_{R,i}$ is the resonance momentum of the ith peak, and m_i and n_i are the constants which have to be determined from the data.

Equation (4.1) actually corresponds to the superposition of Breit-Wigner formulae where $\sigma_b(P_{K,\text{lab}})$ is a nonresonant background. (See refs. 14 and 15.) The fitting constants in the resonance energy range are given in table 4.1. The background functions are fitted by

$$\sigma_b(P_{K,\text{lab}}) = 23.2\ \exp(-0.003 P_{K,\text{lab}}) \tag{4.3}$$

for K^--p scattering and

$$\sigma_b(P_{K,\text{lab}}) = 16.8 - \frac{1}{P_{K,\text{lab}}} \tag{4.4}$$

for K^+-p scattering. When $P_{K,\text{lab}}$ is less than 0.7 GeV/c in K^--p scattering, we used the following function:

$$\sigma_T = 172.38 \ \exp[-2.0(P_{K,\text{lab}} + 0.1)] \tag{4.5}$$

In the more high energy region, the empirical formulae for $K^\pm$-p system are given by

$$\sigma_T = 20.18 + \frac{24.63}{P_{K,\text{lab}}} \tag{4.6}$$

when $P_{K,\text{lab}} > 20$ GeV/c in the K^--p system and

$$\sigma_T = 16.8 - \frac{0.22}{P_{K,\text{lab}}} \tag{4.7}$$

when $P_{K,\text{lab}} > 5$ GeV/c in the K^+-p system. These functions of total cross section are in good agreement with experimental data (refs. 14 and 15) as shown in figures 4.1 and 4.2.

It is easier to parameterize the total cross sections for kaon-nucleus scattering than kaon-proton interaction because the experimental shapes of the former are simpler than the latter. The fitting formulae used are equations (4.8) through (4.11).

For K^--n scattering

$$\sigma_T = -1033.0 + 1060.0 P_{K,\text{lab}}^{-0.03} + 28.0 \ln P_{K,\text{lab}} \tag{4.8}$$

when $P_{K,\text{lab}} \geq 2.5$ GeV/c and

$$\sigma_T = 23.91 + 17.0 \ \exp\left[-\frac{(P_{K,\text{lab}} - 10)^2}{0.12}\right] \tag{4.9}$$

when $P_{K,\text{lab}} < 2.5$ GeV/c.

And for K^+-n scattering,

$$\sigma_T = 18.4 + 175.0 P_{K,\text{lab}}^{-7.85} + 0.2 \ln^2 P_{K,\text{lab}} - 0.75 \ln P_{K,\text{lab}} \tag{4.10}$$

when $P_{K,\text{lab}} \geq 2.5$ GeV/c and

$$\sigma_T = \alpha(18.0 + 3.0 \ \exp\left[-\frac{(P_{K,\text{lab}} - 1.2)^2}{0.08}\right] \tag{4.11}$$

when $P_{K,\text{lab}} < 2.5$ GeV/c. The constant α is equal to 1 when $P_{K,\text{lab}} \geq 1.2$ GeV/c and 0.94 when $P_{K,\text{lab}} < 1.2$ GeV/c.

The equations (eqs. (4.8) and (4.10)) for the high energy region are taken from reference 16. Figures 4.3 and 4.4 display the results of our equations with experimental data taken also from references 16 and 17. In any case, we can anticipate that the resonance bumps will affect the total and absorptive cross sections of kaon-nucleus scattering at the corresponding energies.

4.2. Elastic Slope Parameter

With respect to the shape of the elastic differential cross section, we observe that the rapid falloff of the values of elastic scattering is exponential as t increases. Here $|t|$, which is one of

the convenient Mandelstam variables, is the square value of the momentum transfer. Therefore it has been customary to fit in the small t region with the form

$$\frac{d\sigma}{d\Omega} = C \ \exp(-B|t|) \tag{4.12}$$

which is usually good for $|t| \leq 0.5$ $(\mathrm{GeV}/c)^2$. Here, C is the normalization constant; we call B the exponential slope or slope parameter.

We determined the fitting formulae of the slope parameter in the range of

$$0.1 \leq |t| \leq 0.4 \ (\mathrm{GeV}/c)^2$$

The resultant formulae are shown as follows:

$$B = 7.3 \tag{4.13}$$

for K^--p scattering and

$$B = -24.3 + 7.0 \ \ln(s + 50.0) \tag{4.14}$$

for K^+-p interaction. The invariant mass squared s in units of $(\mathrm{GeV})^2$ is another Mandelstam variable, which represents the square value of the total center-of-mass energy of the system and is related to the kaon laboratory energy ($T_{K,\mathrm{lab}}$ in GeV) as

$$s = m_K^2 + m_N^2 + 2m_N(T_{K,\mathrm{lab}} + m_N) \tag{4.15}$$

where m_K is the projectile kaon mass and m_N is the target nucleon mass.

The results of our slope parameter with experimental data taken from reference 18 are displayed in figures 4.5 and 4.6. The slope parameter for the K^--p system is almost constant, but that for the K^+-p system increases as $T_{K,\mathrm{lab}}$ increases.

4.3. Ratio of Real Part to Imaginary Part of $K^{\pm}$-p Forward Elastic Scattering Amplitude

Our parameterized formulae α for K^--p and K^+-p scattering, respectively, are as follows:

$$\alpha = -\frac{0.32}{1.0 + 0.9P_{K,\mathrm{lab}}^2} \sin\left[\frac{5\pi}{2}(P_{K,\mathrm{lab}} - 0.2)\right] \tag{4.16}$$

for K^--p scattering and

$$\alpha = -1.86 \ \exp\left[-\frac{(P_{K,\mathrm{lab}} - 0.1)^2}{0.41}\right] - 0.44 \tag{4.17}$$

for K^+-p interaction where $P_{K,\mathrm{lab}}$ is the kaon laboratory momentum in GeV/c.

One way to determine the ratio α theoretically is by use of the dispersion relation. The imaginary part of the forward elastic scattering amplitude may be computed in terms of total cross section via the optical theorem:

$$\mathrm{Im}[f(k, \theta = 0)] = \frac{k}{4\pi} \sigma_{\mathrm{total}}(k) \tag{4.18}$$

Then a forward dispersion relation gives the real part of the forward scattering amplitude in terms of an integral over total cross sections. A dispersion relation is defined as an equation which expresses the real part of a function of a complex variable in terms of an integral over the imaginary part (ref. 14). Reference 19 actually gives us the theoretical calculation by the

procedure as mentioned, but the very simple forms of equations (4.16) and (4.17) are sufficient for our purpose.

Figures 4.7 and 4.8 show us our functions and the compilation of the experimental data (ref. 19) for kaon-proton elastic scattering.

Table 4.1. Kaon-Proton Total Cross-Section Fitting Constants

Type of scattering	i	$P_{R,i}$, GeV/c	m_i, mb	n_i, GeV/c
K^--p	1	0.80	11.00	0.21
	2	1.05	27.00	0.20
	3	1.60	9.00	0.35
	4	2.30	4.00	1.00
	5	3.50	4.30	2.00
K^+-p	1	0.80	−4.00	0.40
	2	1.30	2.50	1.00

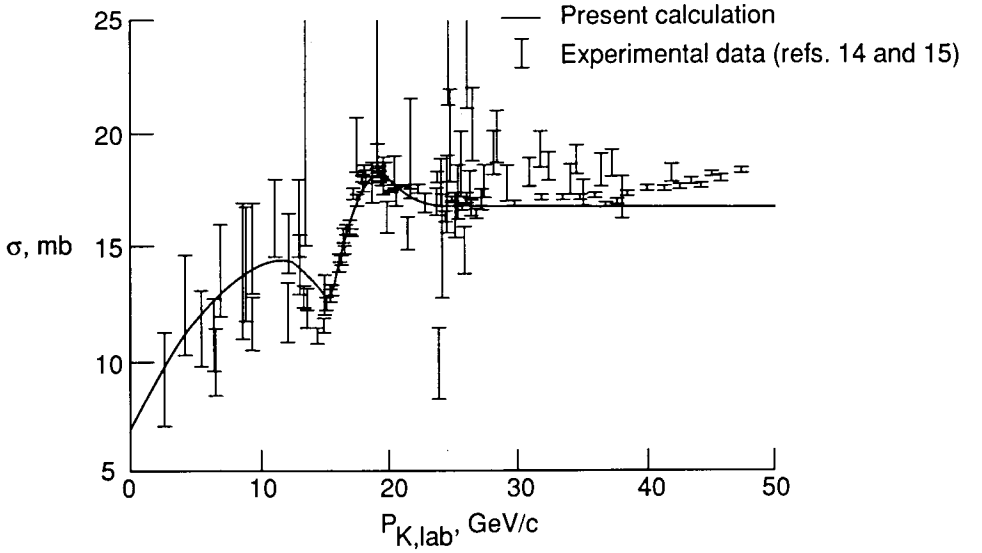

Figure 4.1. Total cross section of K^+-p interaction.

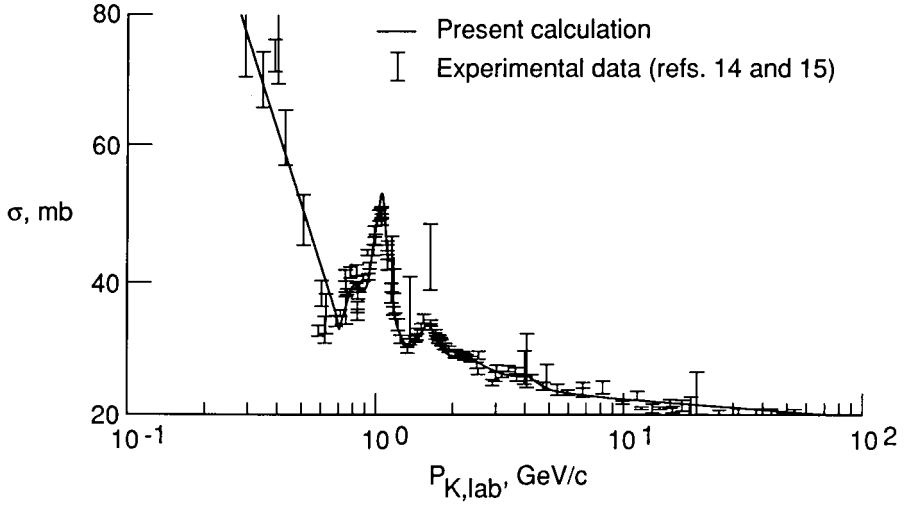

Figure 4.2. Total cross section of K^--p interaction.

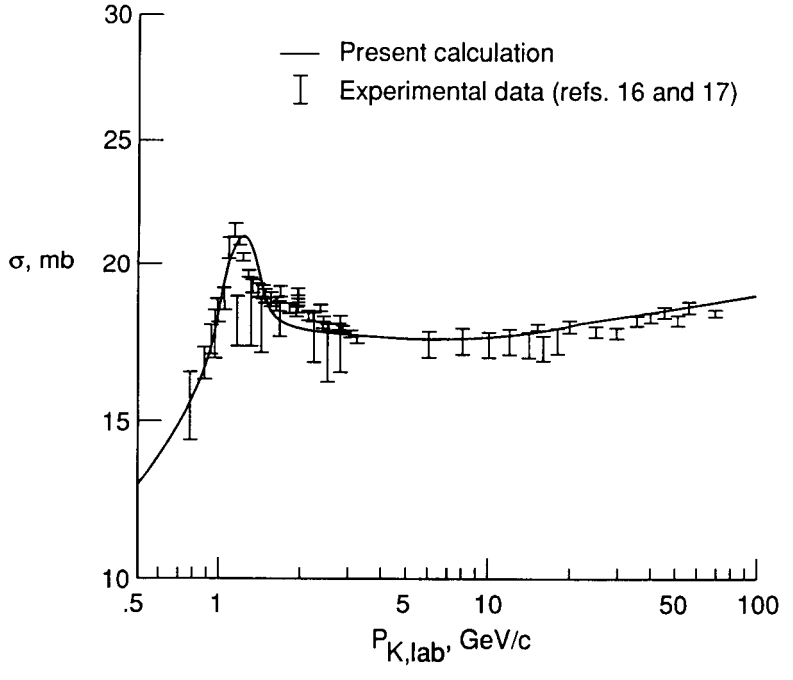

Figure 4.3. Total cross section of K^+-n interaction.

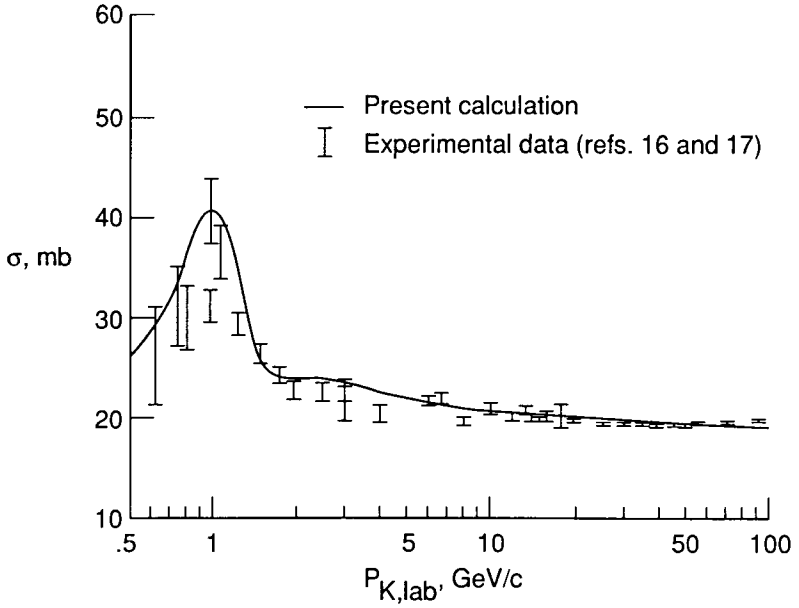

Figure 4.4. Total cross section of K^--n interaction.

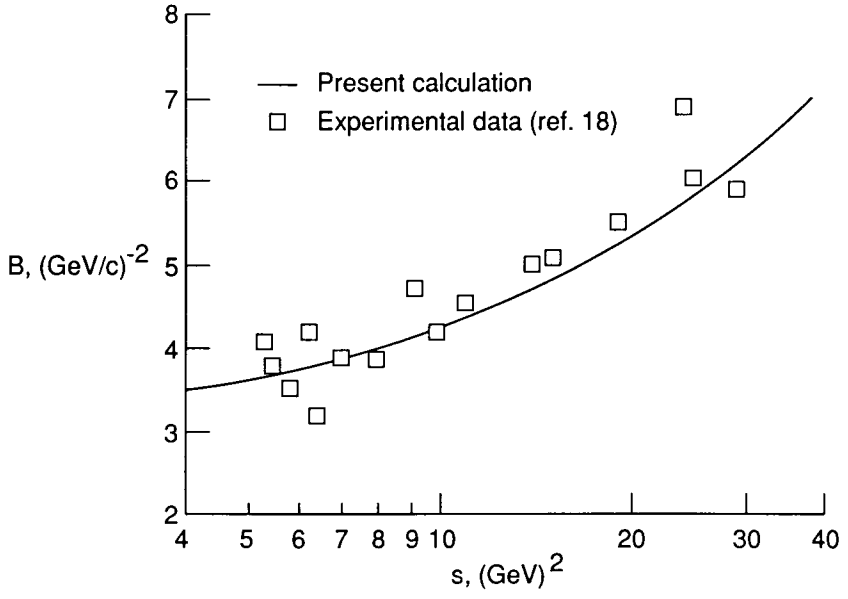

Figure 4.5. Elastic slope parameter of K^+-p interaction in range $0.1 \leq |t| \leq 0.4$ $(\mathrm{GeV}/c)^2$.

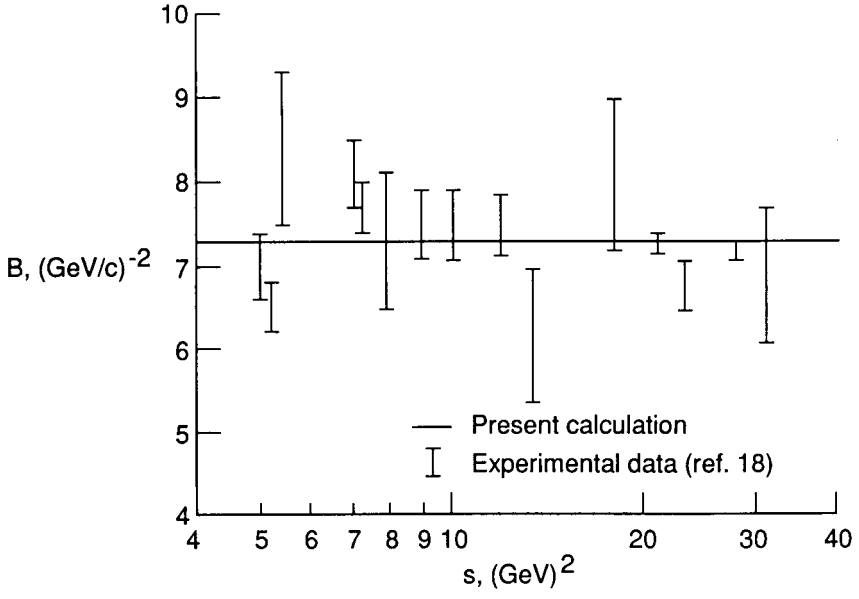

Figure 4.6. Elastic slope parameter of K^--p interaction in range $0.1 \leq |t| \leq 0.4$ $(GeV/c)^2$.

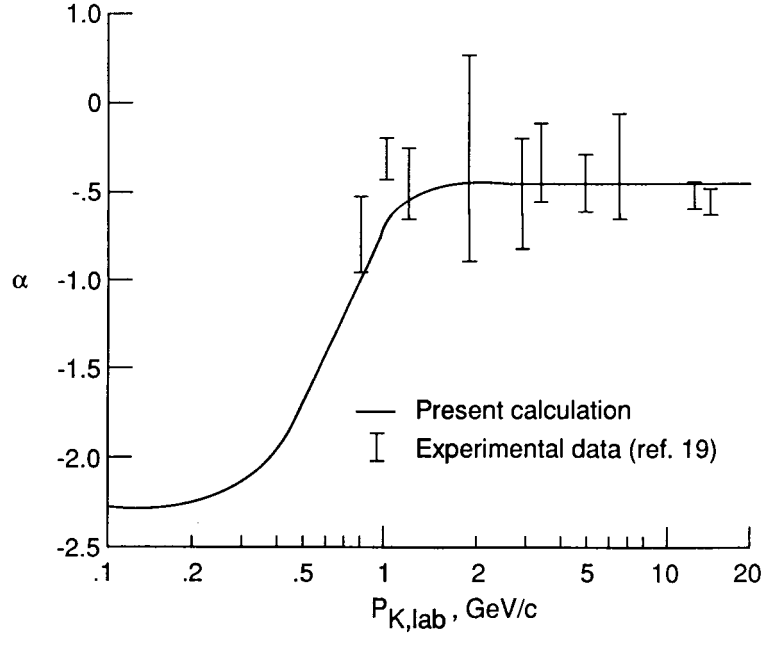

Figure 4.7. Ratio of real to imaginary part of forward elastic scattering amplitude for K^+-p scattering.

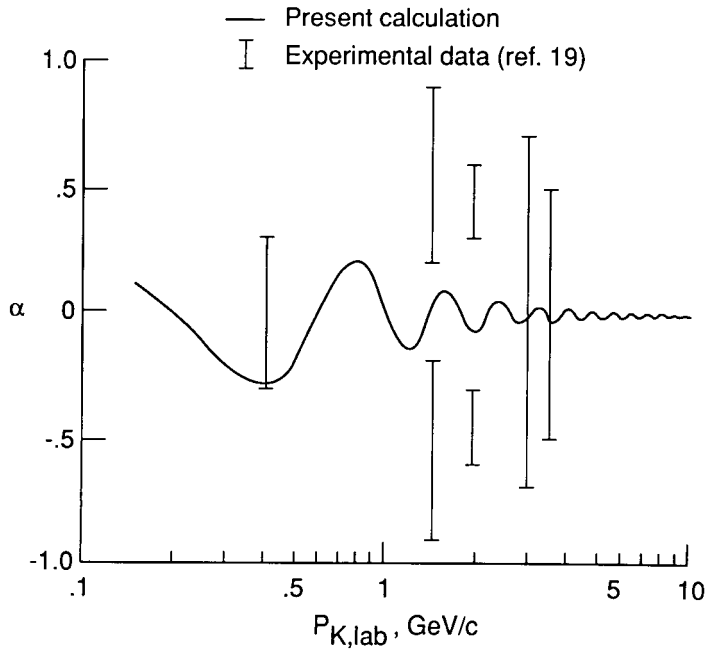

Figure 4.8. Ratio of real to imaginary part of forward elastic scattering amplitude for K^--p scattering.

5. Results

The total and absorptive cross sections for K^+-nucleus scattering using harmonic well and Woods-Saxon single-particle densities are shown in figures 5.1, 5.2, and 5.3 and those for K^- projectile in figures 5.4, 5.5, and 5.6. Although we cannot evaluate the exact error due to the scarcity of experimental data, we expect that the present calculation reasonably represents the situation because of the good agreement between the present calculation and experimental data for other quantities such as the differential cross sections of kaon-proton and kaon-nucleus scattering.

In case of K^+-p scattering, our scattering amplitude was quite reasonable. Moreover, the calculation of the differential cross section gave us more accurate results as the energy of the projectile went higher. For $K^{\pm} - C^{12}$ scattering, the estimated differential cross sections are lower than the experimental results. It may be natural because we used a very simplified, nonrelativistic optical potential. At the very forward angle, the experiments show that the differential cross sections rise very rapidly, but the calculations converge toward smaller values. This comes from the fact that we have neglected the contribution of Coulomb interaction which is the long range interaction in the optical potential.

The total and absorptive cross sections for K^--nucleus scattering were larger than those for K^+-nucleus scattering. This, of course, indicates that the K^- meson interacts more strongly with nucleons than the K^+ meson. According to the quark model, the K^+ resonant peak requires the formation of five quark objects which have never been found, but the kaon-nucleon interactions are so strong that the cross sections are roughly comparable with those of nucleon-nucleon scattering.

The atomic number dependencies of total cross sections are shown in figures 5.7 and 5.8. The K^+-nucleus total cross section shows almost perfect linear dependence on A. The K^--nucleon total cross section also varies linearly with A at high energies but exhibits a little complexity at low energies. We can also note that the absorptive cross section of K^+-nucleus scattering varies linearly with $A^{0.82}$ (fig. 5.9), but the K^--nucleus absorptive cross section does not show as good a linear dependence on $A^{0.82}$ as the total cross section at relatively low energies (fig. 5.10). The linear dependence on $A^{0.82}$ of the absorptive cross section tells us that the nucleus is not perfectly black to the kaon projectile. The analytic fits of this work will be used in the hadron transport computer code at the Langley Research Center (ref. 20).

The advantage of our method to estimate the cross sections is that we can extend it to other scattering systems, for example pion-nucleus scattering, easily knowing the two-body information. Our t-matrix is basically determined by the experimental data, i.e., two-body total cross section, elastic slope parameter, and the ratio of the real part to the imaginary part of the forward scattering amplitude. Therefore if we know all these kinds of information about two-particle scattering, we can calculate differential, total, elastic, and absorptive cross sections.

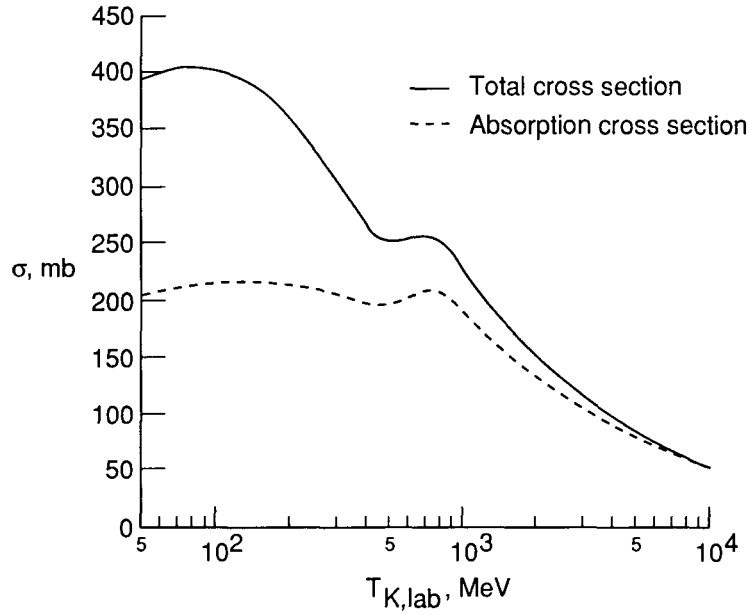

Figure 5.1. Total and absorption cross sections of K^+-Al^{27} scattering according to present calculation.

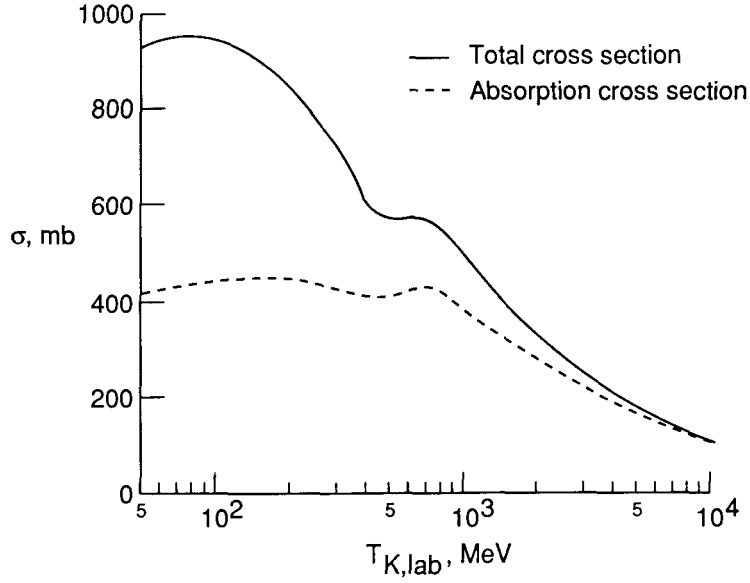

Figure 5.2. Total and absorption cross sections of K^+-Cu^{64} scattering according to present calculation.

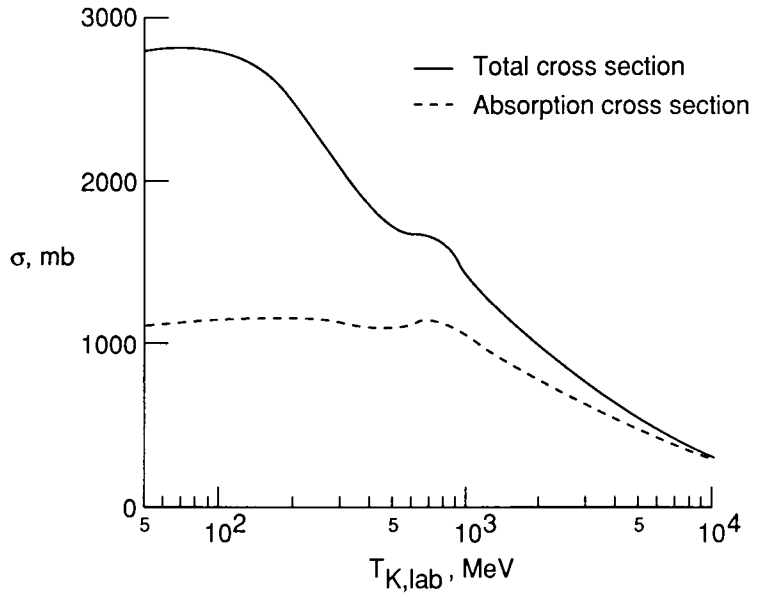

Figure 5.3. Total and absorption cross sections of K^+-Pb^{208} scattering according to present calculation.

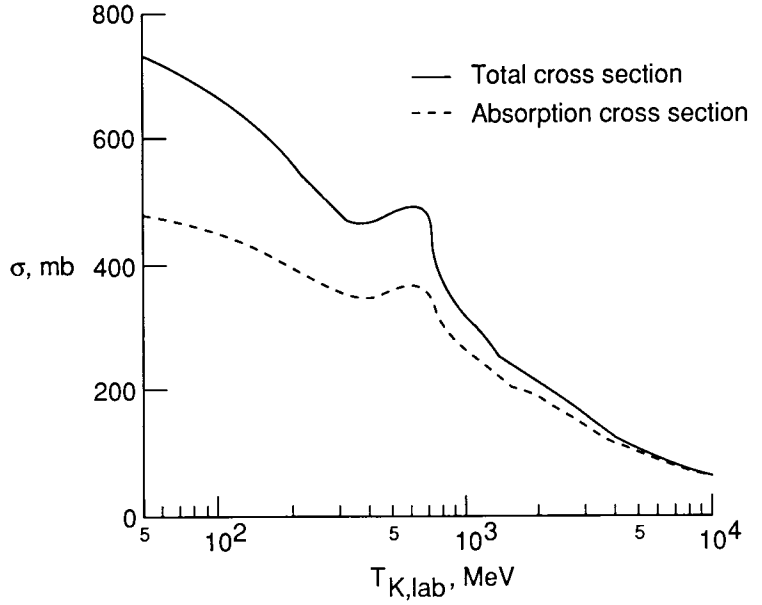

Figure 5.4. Total and absorption cross sections of K^--Al^{27} scattering according to present calculation.

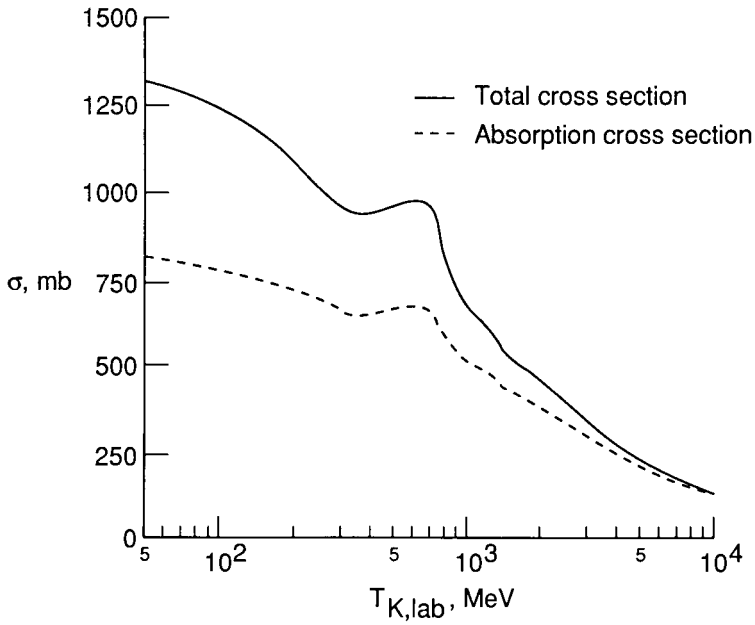

Figure 5.5. Total and absorption cross sections of K^--Cu^{64} scattering according to present calculation.

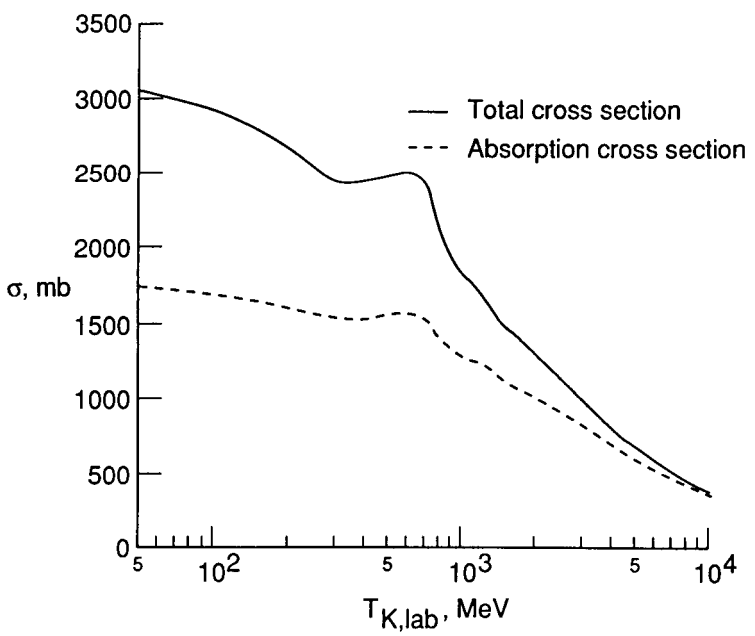

Figure 5.6. Total and absorption cross sections of K^--Pb^{208} scattering according to present calculation.

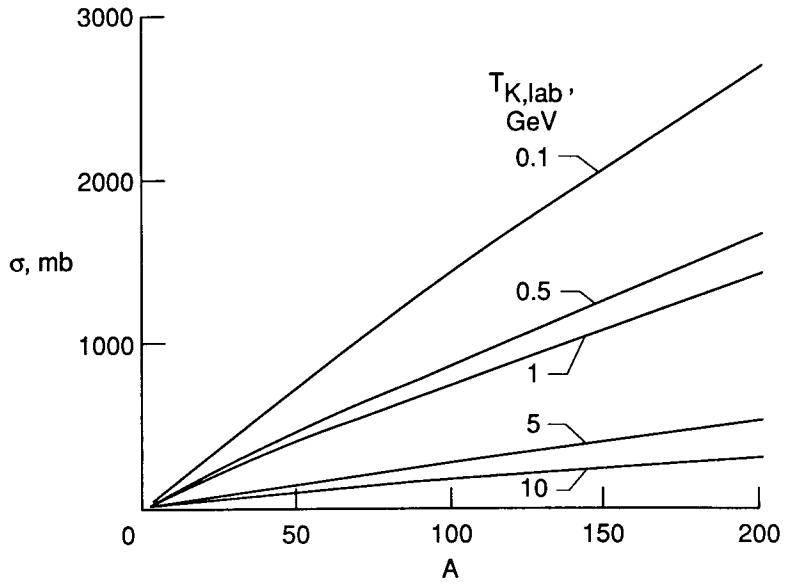

Figure 5.7. Atomic number dependence of total cross section for K^+ projectile.

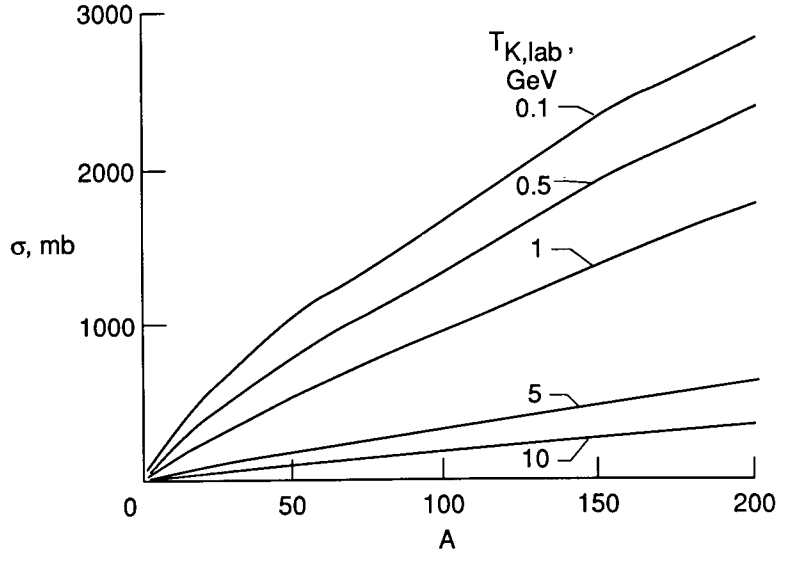

Figure 5.8. Atomic number dependence of total cross section for K^- projectile.

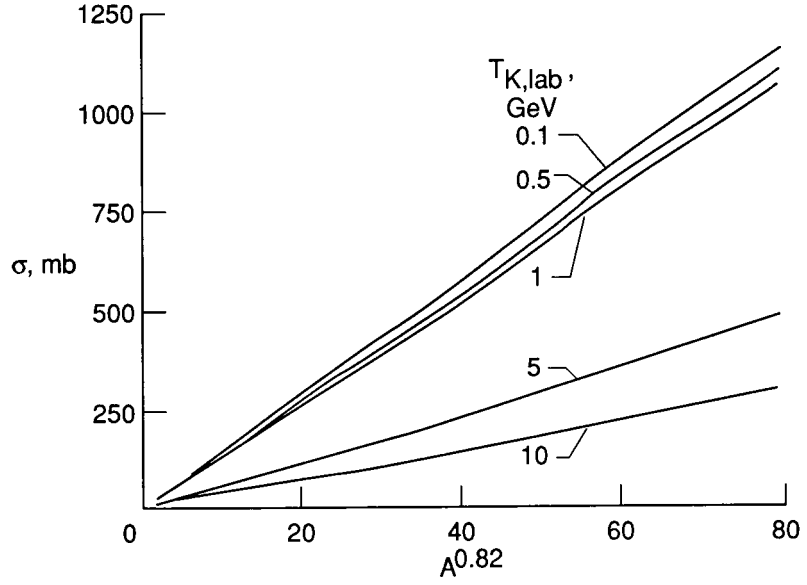

Figure 5.9. Atomic number dependence of absorptive cross section for K^+ projectile.

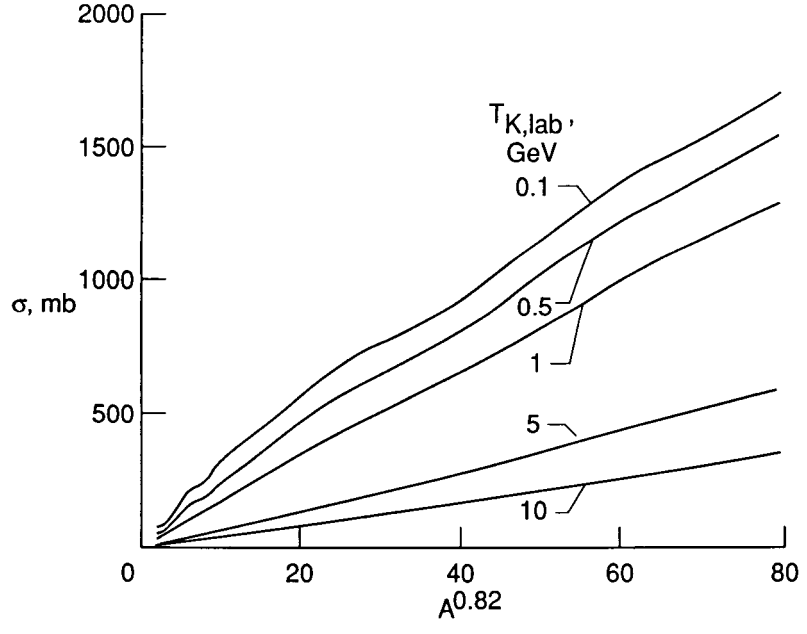

Figure 5.10. Atomic number dependence of absorptive cross section for K^- projectile.

6. Concluding Remarks

The Lippmann-Schwinger equation and the Watson multiple scattering series were derived. Having taken only the first term of that series and having applied the impulse approximation, we obtained a simple optical potential. The number density distribution models of the nucleus,

harmonic well and Woods-Saxon, were used with t-matrix based on the scattering experiments. The parameterized two-body inputs, which are kaon-nucleon total cross sections, elastic slope parameters, and the ratio of the real to the imaginary part of the forward elastic scattering amplitude, were presented. The total and absorptive cross sections for kaon-nucleus scattering were estimated by eikonal approximation. The results of the work will be used in the hadron transport computer code at the Langley Research Center (NASA TP-2887).

NASA Langley Research Center
Hampton, VA 23665-5225
June 1, 1989

References

1. Watson, Kenneth M.: Multiple Scattering and the Many-Body Problem—Applications to Photomeson Production in Complex Nuclei. *Phys. Review,* vol. 89, second ser., no. 3, Feb. 1953, pp. 575–587.
2. Frank, R. M.; Gammel, J. L.; and Watson, K. M.: Optical Model Potential for Pion-Nucleus Scattering. *Phys. Review,* vol. 101, second ser., no. 2, Jan. 15, 1956, pp. 891–901.
3. Watson, K. M.: Multiple Scattering by Quantum-Mechanical Systems. *Phys. Review,* vol. 105, second ser., no. 4, Feb. 15, 1957, pp. 1388–1398.
4. Wilson, John W.: Composite Particle Reaction Theory. Ph.D. Diss., College of William and Mary in Virginia, June 1975.
5. Fernbach, S.; Serber, R.; and Taylor, T. B.: The Scattering of High Energy Neutrons by Nuclei. *Phys. Review,* vol. 75, second ser., no. 9, May 1, 1949, pp. 1352–1355.
6. Wilson, J. W.: Multiple Scattering of Heavy Ions, Glauber Theory, and Optical Model. *Phys. Lett.,* vol. B52, no. 2, Sept. 1974, pp. 149–152.
7. Wilson, J. W.; and Townsend, L. W.: An Optical Model for Composite Nuclear Scattering. *Canadian J. Phys.,* vol. 59, no. 11, Nov. 1981, pp. 1569–1576.
8. Buck, W. W.; Norbury, J. W.; Townsend, L. W.; and Wilson, J. W.: Theoretical Antideuteron-Nucleus Absorptive Cross Sections. *Phys. Review,* vol. 33, third ser., no. 1, Jan. 1986, pp. 234–238.
9. Buck, Warren W.; Wilson, John W.; Townsend, Lawrence W.; and Norbury, John W.: *Possible Complementary Cosmic-Ray Systems: Nuclei and Antinuclei.* NASA TP-2741, 1987.
10. Jackson, Daphne F.: *Nuclear Reactions.* Barnes & Noble, Inc., c.1970.
11. Goldberger, Marvin L.; and Watson, Kenneth M.: *Collision Theory.* John Wiley & Sons, Inc., c.1964.
12. Particle Data Group (LeRoy R. Price, Naomi Barash-Schmidt, Odette Benary, Roger W. Bland, Arthur H. Rosenfeld, and Charles G. Wohl): *A Compilation of* K^+N *Reactions.* UCRL-20000 K^+N, Univ. of California, Sept. 1969.
13. Marlow, D.; Barnes, P. D.; Colella, N. J.; Dytman, S. A.; Eisenstein, R. A.; Grace, R.; Takeutchi, F.; Wharton, W. R.; Bart, S.; Hancock, D.; Hackenberg, R.; Hungerford, E.; Mayes, W.; Pinsky, L.; Williams, T.; Chrien, R.; Palevsky, H.; and Sutter, R.: Kaon Scattering From C and Ca at 800 MeV/c. *Phys. Review,* vol. 25, third ser., no. 5, May 1982, pp. 2619–2637.
14. Giacomelli, G.: Part 2—Total Cross-Section Measurements. *Progress in Nuclear Physics,* Volume 12, D. M. Brink and J. H. Mulvey, eds., Pergamon Press, 1970, pp. 78–225.
15. Bugg, D. V.; Gilmore, R. S.; Knight, K. M.; Salter, D. C.; Stafford, G. H.; Wilson, E. J. N.; Davies, J. D.; Dowell, J. D.; Hattersley, P. M.; Homer, R. J.; O'Dell, A. W.; Carter, A. A.; Tapper, R. J.; and Riley, K. F.: Kaon-Nucleon Total Cross Sections From 0.6 to 2.65 GeV/c. *Phys. Review,* vol. 168, no. 5, Apr. 25, 1968, pp. 1466–1475.
16. Baldini, A.; Flaminio, V.; Moorhead, W. G.; and Morrison, D. R. O.: *Total Cross-Sections for Reactions of High Energy Particles. Landolt-Börnstein Numerical Data and Functional Relationships in Science and Technology,* Group I, Volume 12a, H. Schopper, ed., Springer-Verlag, c.1988.
17. Baldini, A.; Flaminio V.; Moorhead, W. G.; and Morrison, D. R. O.: *Total Cross-Sections for Reactions of High Energy Particles. Landolt-Börnstein Numerical Data and Functional Relationships in Science and Technology,* Group I, Volume 12b, H. Schopper, ed., Springer-Verlag, c.1988.
18. Perl, Martin L.: *High Energy Hadron Physics.* John Wiley & Sons, Inc., 1974.
19. Lusignoli, M.; Restignoli, M.; Violini, G.; and Snow, G. A.: Comparison of $K^{\pm}p$ Dispersion Relations With Experiment. *Nuovo Cimento Soc. Italiana Fis. A,* vol. XLV, no. 3, Oct. 1, 1966, pp. 792–798.
20. Wilson, John W.; Townsend, Lawrence W.; Nealy, John E.; Chun, Sang Y.; Hong, B. S.; Buck, Warren W.; Lamkin, S. L.; Ganapol, Barry D.; Khan, Ferdous; and Cucinotta, Francis A.: *BRYNTRN: A Baryon Transport Model.* NASA TP-2887, 1989.

NASA
National Aeronautics and Space Administration

Report Documentation Page

1. Report No.	2. Government Accession No.	3. Recipient's Catalog No.
NASA TP-2920		

4. Title and Subtitle	5. Report Date
Kaon-Nucleus Scattering	July 1989
	6. Performing Organization Code
7. Author(s)	8. Performing Organization Report No.
Byungsik Hong, Khin Maung Maung, John W. Wilson, and Warren W. Buck	L-16583
9. Performing Organization Name and Address	10. Work Unit No.
NASA Langley Research Center Hampton, VA 23665-5225	199-22-76-01
	11. Contract or Grant No.
12. Sponsoring Agency Name and Address	13. Type of Report and Period Covered
National Aeronautics and Space Administration Washington, DC 20546-0001	Technical Paper
	14. Sponsoring Agency Code

15. Supplementary Notes

Byungsik Hong, Khin Maung Maung, and Warren W. Buck: Hampton University, Hampton, Virginia.
John W. Wilson: Langley Research Center, Hampton, Virginia.

16. Abstract

The derivations of the Lippmann-Schwinger equation and the Watson multiple-scattering series are given. A simple optical potential is found to be the first term of that series. The number density distribution models of the nucleus, harmonic well and Woods-Saxon, are used with our t-matrix taken from the scattering experiments. The parameterized two-body inputs, which are kaon-nucleon total cross sections, elastic slope parameters, and the ratio of the real to the imaginary part of the forward elastic scattering amplitude, are presented. The eikonal approximation was chosen as our solution method to estimate the total and absorptive cross sections for the kaon-nucleus scattering.

17. Key Words (Suggested by Authors(s))	18. Distribution Statement
Kaon interactions Nuclear reactions Optical model Multiple scattering	Unclassified—Unlimited Subject Category 93

19. Security Classif. (of this report)	20. Security Classif. (of this page)	21. No. of Pages	22. Price
Unclassified	Unclassified	29	A03

NASA-Langley, 1989

For sale by the National Technical Information Service, Springfield, Virginia 22161-2171